A Robust Method for Assessing 3-D Topographic Site Effects: A Case Study at the LSBB Underground Laboratory, France

Emeline Maufroy,[a)] Víctor M. Cruz-Atienza,[b)] and Stéphane Gaffet[a,c)]

By means of three-dimensional (3-D) numerical simulations, including the Laboratoire Souterrain à Bas-Bruit (LSBB) topography, we carefully analyze site effects assessments yielded by two approaches: the classical site to reference spectral-ratio method (SRM) and the statistical median reference method (MRM). We show for both isotropic and double-couple point sources that a 94% reduction in the number of stations of a regularly spaced array yields MRM site-effect estimates within 5% of those obtained from the absolute regional median, and within 20% using a 98% station reduction with irregularly located sites. In contrast, the SRM yielded site-effect overestimates greater than 50% in some areas and up to 100% in specific sites, which makes the MRM much more robust than the SRM. We determined a 33% probability to exceed an amplification factor of 2, and an 8% probability to exceed a factor of 3 due to topography in the surroundings of the sharpest summit of the LSBB area. [DOI: 10.1193/1.4000050]

INTRODUCTION

Surface topography is known to significantly affect ground motion due to the incidence of seismic waves. Numerous observations during strong earthquakes have shown a higher level of damage on the top of hills, as compared to the levels observed on flat grounds or hollow topographies (Trifunac and Hudson 1971, Boore 1972, Çelebi 1987, Kawase and Aki 1990, Spudich et al. 1996, Bouchon and Barker 1996, Assimaki et al. 2005a). This so-called topographic site effect has been regularly recorded ever since its first description (Boore 1972, based on the observations from Trifunac and Hudson 1971). The highest topographic regions are mostly affected by an amplification of the ground motion in a frequency band, which depends on the characteristic dimension of the relief (Boore 1972, 1973, Bouchon 1973, Durand et al. 1999). This frequency band often ranges from 1 Hz to 20 Hz, thus containing frequencies typically considered for paraseismic structural design.

This phenomenon is of great concern for the seismic hazard assessment in mountainous areas. The topographic site effect has been qualitatively well described. However, quantitative ground motion predictions including the topographic site effects within the proper frequency band remains a challenge for the research community (Geli et al. 1988, Bouchon and

[a)] GEOAZUR, UMR 7329, Université de Nice Sophia-Antipolis, CNRS, Observatoire de la Côte d'Azur, Sophia-Antipolis, 06560 Valbonne, France
[b)] Instituto de Geofísica, Universidad Nacional Autónoma de México. 04510 México D.F., Mexico
[c)] LSBB, UMS Université de Nice Sophia-Antipolis, Université d'Avignon et des Pays de Vaucluse, CNRS. La grande combe, 84400 Rustrel, France

Earthquake Spectra, Volume 28, No. 3, pages 1097–1115, August 2012;

Barker 1996, Ashford and Sitar 1997). Numerous studies have been performed on this topic; yet no general agreement exists about the method to use (Chávez-García et al. 1996, 1997). There is also no agreement about the importance of this phenomenon: some authors tend to consider the topographic site effect as a first order one (Davis and West 1973, Tucker et al. 1984, Geli et al. 1988, Umeda et al. 1987, Bard and Méneroud 1987, Gaffet et al. 2000), while others disagree (Rogers et al. 1974, Pedersen et al. 1994).

Such controversy is mainly due to the discrepancies between the predicted and observed amplification levels. Ground motion simulations with topography have been conducted since the phenomenon was first described in 1972 (Boore 1972). Nevertheless, the predicted amplification levels often underestimate the observations (Geli et al. 1988, Bouchon and Barker 1996, Sanchez-Sesma and Campillo 1991). Amplification is commonly expressed in terms of the spectral ratio between the waves amplitude at the top (assumed as maximal) and at the bottom (assumed as not amplified) of a hill. In the frequency band of interest, the calculated ratios rarely exceed 2 (Boore 1972, Bouchon 1973, Wong 1982, Kawase and Aki 1990, Pedersen et al. 1994, Bouchon and Barker 1996, Assimaki et al. 2005a, 2005b), while the observed ratios very often exceed this threshold and may reach up to 10 (Davis and West 1973, Geli et al. 1988, Umeda et al. 1987, Bard and Méneroud 1987, Gaffet et al. 2000). Some authors attributed such discrepancies to the fact that the medium was described in 2-D (Geli et al. 1988, Bouchon and Barker 1996). 3-D ground motion calculations certainly tend to decrease the disparity between predicted and observed spectral ratios (Lee et al. 2009a, 2009b, Chaljub et al. 2010; this paper). Another major obstacle to quantify the topographic site effect comes from the strong coupling between the topography and local geology that may affect the seismic wavefield with similar intensity (Wong et al. 1977, Assimaki et al. 2005a). If the effects from both agents are comparable and we lack of knowledge about the local geology, it becomes impossible to quantify the topographic site effect separately (Hartzell et al. 1994).

Despite all previous investigations, it is still difficult to compare site effect assessments for different topographic study cases. The strategy most commonly used to calculate the topographic site effect is the site-to-reference spectral ratio method (single reference method, SRM; Davis and West 1973, Tucker et al. 1984, Bard and Méneroud 1987, Çelebi 1987, Umeda et al. 1987, Pedersen et al. 1994, Nechtschein et al. 1995, Gaffet et al. 2000). This method is easy and fast, adequate to real data, and doesn't need a high number of stations. However, this method requires the definition of a reference site, which is not affected by site effects. Some authors point out that the perfect reference site does not exist (Tucker et al. 1984, Chávez-García et al. 1996, Steidl et al. 1996). Numerous studies use the foot of the hill as the reference site (Bard and Méneroud 1987, Geli et al. 1988, Pedersen et al. 1994), even if the wavefield there may be affected by a topographic deamplification (Bouchon 1973, Nechtschein et al. 1995). The choice of the reference site is critical. If not suitable, it can lead to either overestimate or underestimate the amplification factors at the top of hills (Tucker et al. 1984, Geli et al. 1988). Therefore, since each study has its own reference site, it is misleading to compare estimates of topographic site effects obtained in different regions of interest. To overcome this problem, some authors performed numerical simulations of the ground motion considering the outcome seismograms from a flat topography as the reference (Boore 1972, Bouchon 1973, Boore et al. 1981, Wong 1982, Bouchon and Barker 1996, Lee et al. 2009a, 2009b). This reference can be considered as absolute but is not rigorously

realistic. Therefore comparison between observed and predicted site effect estimates remains a difficult and delicate matter.

Wilson and Pavlis (2000) have introduced a statistical spectral ratio method (median reference method, MRM). The reference is no longer a specific site, but a measure over the whole studied area. If the area contains a wide variety of topographic features (e.g., hills, slopes and hollows), the reference becomes a regional measure that can be considered as the median ground motion of the mountainous area. Site effects are thus present in specific subareas where the amplitude of ground motion differs from the median reference one. They used the MRM on a flat hard rock site, while Poppeliers and Pavlis (2002) applied it on a regular slope. In both studies, the areas of interest were small (i.e., of the order of 2000 m^2) and were covered by very dense seismic arrays (i.e., interspacing of ~10 m). Their results showed the efficacy of the MRM at a very local scale provided such optimal instrumentation conditions. Whether this technique remains robust under different and more likely conditions for seismological purposes (e.g., with irregular topography and sparse seismic arrays) still is an open question.

In this study, we further investigate the MRM and present interesting insights about its performance. We show that the MRM is a very powerful tool for the assessment of site effects on complex and steep topographies, particularly when the definition of a reference site is difficult or arbitrary. We also show that the MRM is remarkably robust regardless of the amount of seismic stations, allowing the comparison of site effects between different study cases. We perform a systematic and quantitative comparison of results with those from the SRM to conclude that the MRM is substantially more stable. Such comparison illustrates as well other advantages of the statistical approach, which makes the choice of a reference a much easier and reasonable task.

Although the coupled effect of both local geology and topography may not be dissociated in real data, for the sake of clarity, results in this study correspond to 3-D ground motion simulations within a homogeneous halfspace overlaid by an irregular topography. To reliably assess the topographic site effect, we thus exclude any particular effect due to geological heterogeneities inside the massif. In this paper we focus on the geometrical effects produced by the morphology of the free surface, which is a major source of problems for the SRM. We show that these problems can be overcome by using the MRM. Our simulations were done with the SHAKE3D finite-difference code (Cruz-Atienza et al. 2007a, 2007b), which allows modeling the propagation of seismic waves in complex 3-D media with realistic surface topography. We used a high-resolution digital map of the ground topography of the area where the inter-Disciplinary Underground Science and Technology Laboratory (i-DUST, LSBB, France, http://lsbb.oca.eu) is located.

TWO METHODS FOR ESTIMATING THE TOPOGRAPHIC SITE EFFECT

THE SINGLE REFERENCE METHOD (SRM)

The most classical and commonly used method to quantify the site effects in mountainous areas is the site-to-reference spectral ratio method (Borcherdt, 1970), hereafter referred to as the SRM.

To isolate the effects associated with the topography from other effects affecting the seismic wavefield, recordings in two separated sites are required. The SRM assumes that the only difference between these recordings is due to the coupled effect of the topography and the local geology, which should not be present in one of the sites, the so-called reference site. All other factors determining the wavefield are assumed to be the same in all recordings (Davis and West 1973, Field and Jacob 1995).

Following Davis and West (1973), the ground motion recorded at a station i on the component j from a source k may be defined as:

$$A_{ijk}(\omega) = S(\omega)\, P_{ijk}(\omega)\, T_{ijk}(\omega)$$

where $S(\omega)$ is the source function, $P_{ijk}(\omega)$ is the regional Earth-propagation transfer function between the source and the area of interest, and $T_{ijk}(\omega)$ is the site effect transfer function including both the topography and local geology effects in the receiver position.

By assuming that $S_{ref.}(\omega) \approx S_p(\omega)$, $P_{ref.jk}(\omega) \approx P_{pjk}(\omega)$ and $T_{ref.jk}(\omega) \approx 1$ (Davis and West 1973), the site effect function $T_{pjk}(\omega)$ at point p can be approximated as:

$$T_{pjk}(\omega) = \frac{A_{pjk}(\omega)}{A_{ref.jk}(\omega)} \tag{1}$$

where the subscript *ref.* means "at the reference site". Most hypotheses mentioned above may be fine when using small-aperture arrays, except for the following two: (1) $P_{ref.jk}(\omega) \approx P_{pjk}(\omega)$, which requires the reference site to be close enough to p; and (2) $T_{ref.jk}(\omega) \approx 1$, which requires that the reference site does not experience the site effects present at p due to both topography and local geology. Both hypotheses may not be satisfied simultaneously since the second one requires the reference site to be far away from p, because the area affected by the topography is larger than the dimensions of the massif (Pedersen et al. 1994, Chávez-García et al. 1996). Such experimental configuration is certainly unlikely to exist in the field. The hypotheses behind the SRM thus require exceptional experimental configurations so that both antithetic conditions are reasonably well satisfied simultaneously.

THE MEDIAN REFERENCE METHOD (MRM)

Wilson and Pavlis (2000) introduced a statistical approach involving the median of the spectral ratios for a given stations array. Spectral ratios are calculated for all possible couples of stations, disregarding their locations. A statistically determined amplification factor at a given station may be thus obtained by calculating the median value of all ratios between this station and all the others (including itself). The site effect transfer function $T_{ijk}(\omega)$ (see previous section) at a station i on the component j from a source k is then expressed as:

$$T_{ijk}(\omega) = median\left(\frac{A_{ijk}(\omega)}{l = 1, 2, \ldots, N_{lk}[A_{ljk}(\omega)]}\right) \tag{2}$$

where N_{lk} is the number of the stations in the seismic array that recorded the event k (Wilson and Pavlis 2000).

The MRM simplifies the choice of a reference since all stations are taken into account. The reference becomes the median spectrum of the array and is not anymore a single site somehow chosen arbitrarily. This median spectrum thus represents a characteristic function holding the common part of the ground motion that is present all over the area covered by the seismic array. In the following we illustrate the accuracy and robustness of this statistical approach. We shall see as well that site effects estimated from both the MRM and SRM become strictly equivalent when the reference site is correctly chosen in the SRM.

3-D FINITE-DIFFERENCE MODELING OF THE TOPOGRAPHIC SITE EFFECT

Simulations in this study were done using the SHAKE3-D partly staggered finite-difference code (Cruz-Atienza 2006), initially developed to simulate the dynamic rupture of earthquakes in complex media (Cruz-Atienza et al. 2007a). The code simulates an infinite halfspace by applying perfectly matched layer (PML) absorbing boundary conditions in every external limit of the computational domain (see Cruz-Atienza 2006 and references therein). To integrate the surface topography in our simulations we use the vacuum-formalism technique at the top of the model, which verifies accurately the free-surface boundary conditions provided that 60 grid points per minimum wavelength are guaranteed everywhere over the surface topography (Bohlen and Saenger 2006). The elastic and isotropic medium is entirely described in every grid point by the density ρ and both the P- and S-wave speeds, denoted as V_P and V_S respectively. In our analysis, we considered both isotropic and double-couple point sources with a Gaussian-like time evolution by adding the equivalent distribution of body forces to the equation of motion (Cruz-Atienza et al. 2007b).

In order to study separately the topographic site effect we assumed, for all simulations, the same homogeneous elastic model with properties given by $V_P = 5.0$ km/s, $V_S = 3.0$ km/s and $\rho = 2.6$ g/cm^3. This implies that the site effect transfer function, $T_{ijk}(\omega)$ (Equations 1 and 2), which in general involves the coupled effect of both topography and local geology, only consists of the topographic site effect. The free surface geometry corresponds to the high-resolution topographic map of the LSBB site. The model is discretized with a grid size of 10 m, which guarantees a good numerical accuracy for frequencies lower than 5 Hz (Bohlen and Saenger 2006). Wave propagation simulations were run in a model with dimensions $5 \times 5 \times 7$ km^3 and a propagation time of 5 s. They required ~12 Gb of RAM memory and a computational time ranging from 20 to 72 hours depending on the computer power.

The choice of isotropic and double-couple point sources within a homogeneous model means that we solve for P, SH, and SV incident and reflected waves, as well as for non-dispersive Rayleigh trains along the free surface. In our model, the topographic site effect only depends on the source-topography configuration. As we shall see, our analysis lead us to essentially the same conclusions whatever the kind of source we take. To illustrate our simulations, Figure 1 shows the model topography along with some synthetic waveforms computed for an isotropic source (i.e., only P incident waves) at four different but closely located sites. Note the strong differences in peak velocities and waveforms that are essentially due to the surface topography. The topographic site effect is thus clearly observed in the amplitudes, which may differ by a factor of three between two neighboring stations (Figure 1c). In both

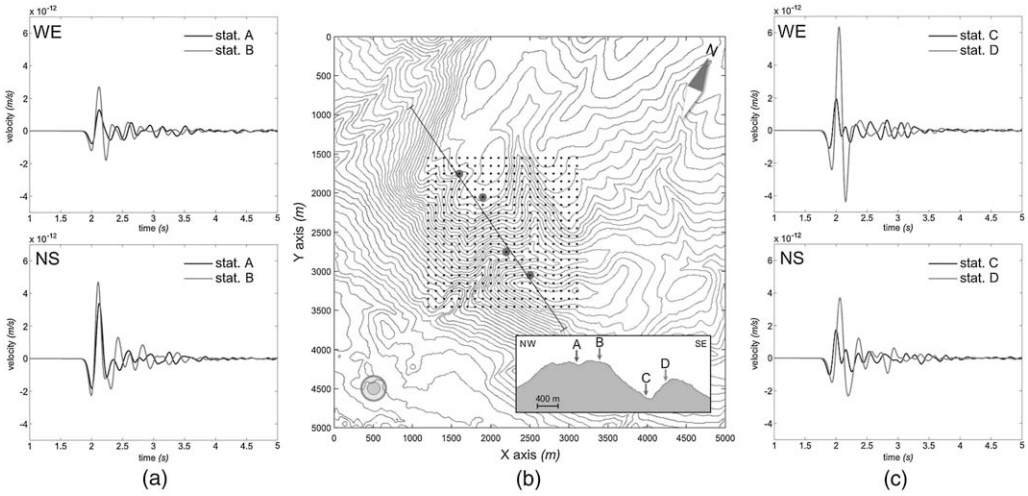

Figure 1. An example of waveforms calculated with the Shake3D finite-difference code for an array of 400 stations (small black dots) covering the area of the LSBB Underground Laboratory site. The 3-D digital map of the topography was used in the calculations (level contours every 20 m). The positions of the stations A, B, C and D are indicated in (b) by the gray-black dots. Waveforms are compared between pairs of stations to illustrate the topographic effect on the wavefield (a and c). We considered a 5 km depth isotropic source located at the southwestern-corner of the model.

couples of neighboring stations, A-B and C-D, we find that the higher the site elevation, the higher is the peak velocity. Our results at station A (Figure 1a) illustrate furthermore the possibility of obtaining relatively smaller amplitudes at sites located over an overall elevated region, but within a smaller scale valley (see Figure 1b).

ANALYSIS OF A STUDY CASE: THE LSBB SITE

Figure 2 presents site effect assessments from both the SRM and MRM. In this section we consider both isotropic and double-couple point sources along with a dense seismic array consisting of 400 equidistant stations covering a variety of topographic features (black dots on Figure 2a), including elevated areas and valleys surrounding the LSBB. The array thus partly covers the Albion plateau and the Apt basin edge. Such topographic features have different orientations and steepness. The source (indicated by the red circle on Figure 2a) is located to the southwest of the array at 5 km depth.

MRM SITE EFFECT ESTIMATES

Figure 2b shows the distribution of single-reference spectral-ratio values (i.e., SRM site-effect estimates, Equation 1) over the whole seismic array for three stations: R, V, and S. Each panel shows the SRM estimates per station (i.e., stations R, V, and S represent the site p in Equation 1) taking as reference site (i.e., as the site *ref*.) each one of the 400 stations in the

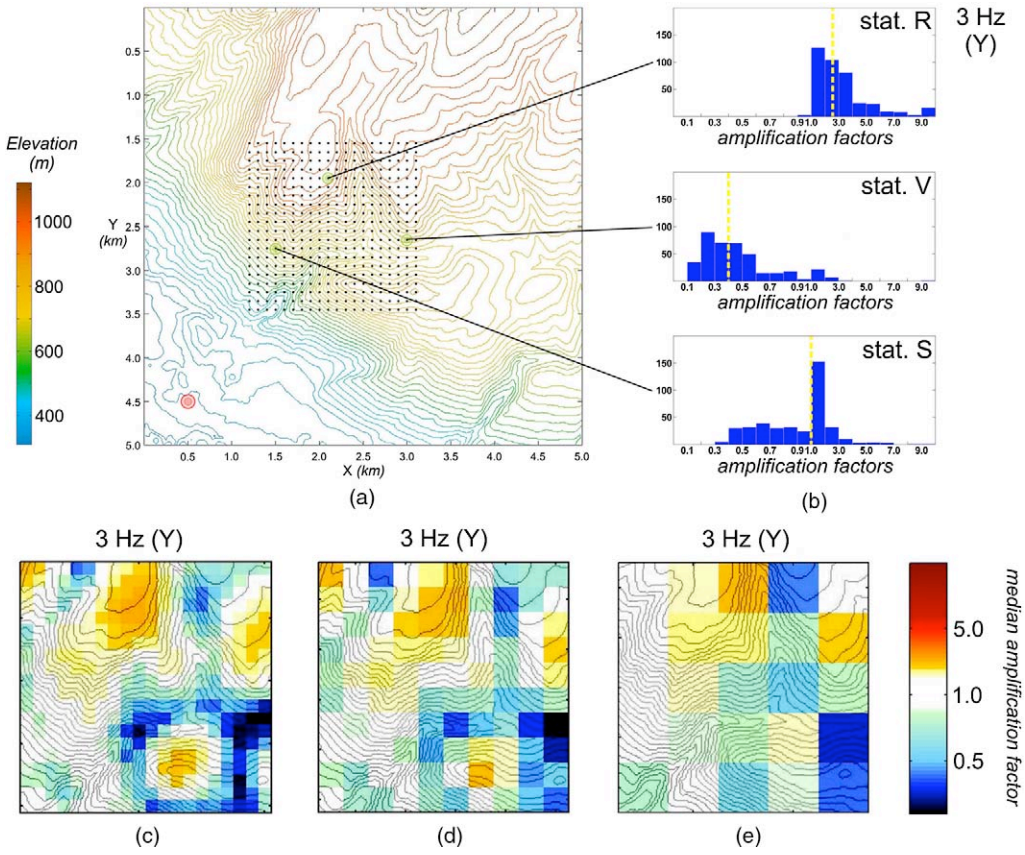

Figure 2. (a) LSBB topographic model covered by a regular dense array of the stations (black dots). Elevation contour lines are every 20 m. The isotropic source (red circle) is 5 km depth. (b) Distribution of single-reference spectral ratios obtained at three array stations, R, V and S (green circles in a). MRM amplification factors (displayed as colored pixels) are computed for three arrays consisting of (c) all 400 stations, (d) 100 stations and (e) 25 stations. Arrays used in (d) and (e) were built from the full array by decimating it every 4 and 16 stations respectively. MRM estimates were performed for the frequency of 3 Hz along the Y component.

array. The y-axes are the amount of spectral ratios per estimated value of the SRM at 3 Hz in the Y (North-South) component. The distributions obtained at stations located in both a ridge and a valley (stations R and V) are not Gaussian. They thus suggest that the more suitable statistical procedure to estimate the amplification factor in these sites is not the average but the median of the ground motion (i.e., the MRM, yellow dashed lines in Figure 2b). Another statistical approach was proposed by Montalvo-Arrieta et al. (2002). They used the average spectra to define a virtual reference site for Mexico City. However, as discussed above, our results indicate that using the average spectra would overestimate the MRM amplification factors. On the other hand, stations located in non-amplified areas typically present a well-defined unimodal distribution (e.g., station S on Figure 2b), with most of the

amplification factors concentrated between 1.0 and 2.0, which implies a median equal to 1 (i.e., no amplification effect).

To analyze the robustness of the site effect estimates using the MRM (Equation 2) we performed calculations for three different but regularly spaced arrays consisting of 400 stations (Figure 2c), 100 stations (Figure 2d) and 25 stations (Figure 2e). To better appreciate the ground motion behavior in the whole area, the MRM amplification factors at 3 Hz computed in each array are superimposed on the topography. Figure 2c clearly reveals a spatial correlation between the MRM amplification factor pattern and the topography. In general, high amplification factors cover elevated areas (e.g., ridges) while low factors coincide with lower areas (e.g., valleys). In this particular simulation, the MRM factors can reach values up to 3.6, but remain typically around 2.5 in the amplified areas. These values are in the same range as those obtained from other studies (summarized in Geli et al. 1988). Deamplifications are observed along the valleys and are of the same order as the amplification on the ridges.

Figures 2c-e also show that the amplification pattern remains stable regardless of the number of the stations considered in the calculations (e.g., compare Figures 2d and 2e). Figure 3 presents the MRM amplification factors in 25 stations computed with the three different array densities. Discrepancies between estimates in all stations are within the

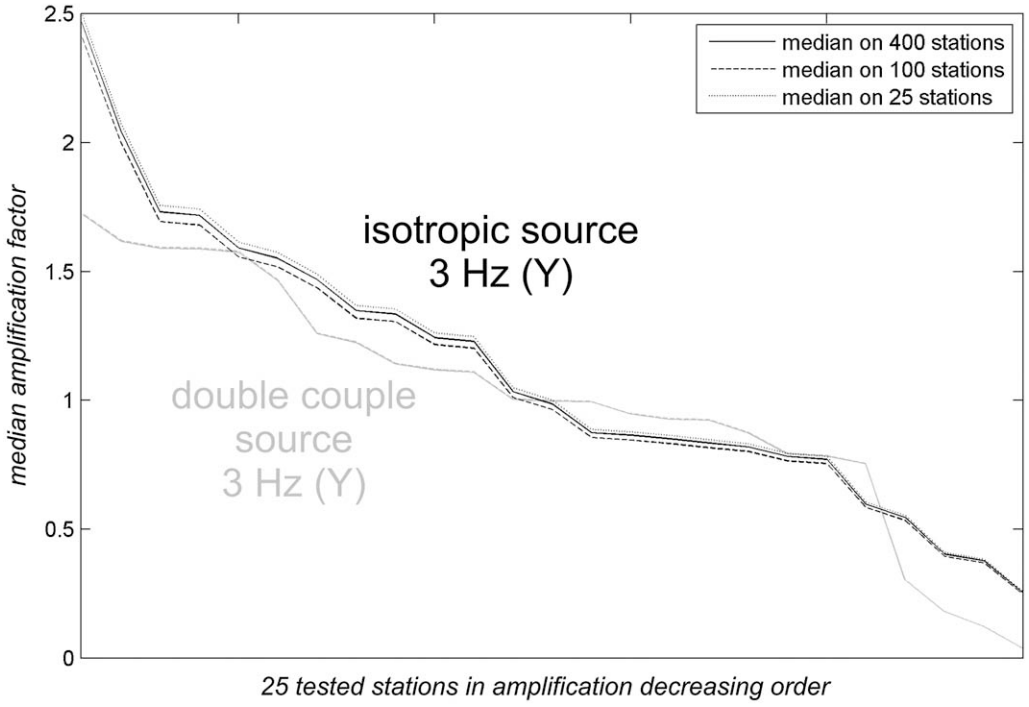

Figure 3. MRM amplification factors obtained for 25 selected stations by using the median calculated on: all 25 stations (dotted line), 100 stations (dashed line) and 400 stations (solid line), considering both isotropic (black lines) and double couple (gray lines) sources.

5% of the values obtained using 400 stations (solid black line), which proves the robustness of the MRM technique in assessing the topographic site effect. If the array covers the studied area properly, the stations density has a weak influence on the MRM amplification factors. A high-density array may be useful to obtain a high-resolution map of the MRM site effects (Figure 2c). A lower amount of stations leads to a low-resolution map (Figure 2e), which still contains reliable information about the topographic site effect, as demonstrated by Figure 3.

In order to test whether the robustness of the method depends on the kind of seismic source, we have performed the same exercise but considering a double-couple point excitation with an arbitrary chosen focal mechanism (i.e., strike = 300°, dip = 45°, and rake = −150°). Figure 3 (gray lines) shows that the kind of seismic radiation (i.e., P and S incident waves) does not have any influence at all in the robustness of the MRM. Whatever the array density is, we find virtually the same amplification factors in all selected stations. Either an isotropic or a double-couple source, the amount of seismic stations in a regularly distributed array does not play a relevant role in the MRM site-effect assessment. As expected, the absolute amplification factors are different from one source to the other (compare black and gray lines), illustrating how the mechanism of the source cannot be dissociated from the topographic site-effect pattern.

COMPARISON BETWEEN THE SRM AND THE MRM

To compare the performance of the MRM and SRM techniques, let us consider an array with a number of stations likely to be available in the field. The number of stations is often small. Let us consider only 8 stations spread out over our topographic model in a suitable way to sample an a priori interesting ridge effect (Figure 4). In the case of the SRM, we will take as reference those sites lying within a valley (i.e., stations 3 and 8). This choice is critical but partly justified a priori since these stations are located in the lowest topographic spots, between the two main hills (station 3), and at the foot of the Albion plateau (station 8), which is the main topographic feature in the area (Figure 4).

Taking station 3 as the reference site, the SRM yields the site-effect estimates indicated with circles in Figure 5. We find a maximum amplification factor of 2.4 at station 1, located on a sharp crest. If station 8, located at the foot of the Albion plateau, is now taken as the reference site (triangles in Figure 5), calculations predict no deamplification (i.e., all amplification factors are bigger than one) and a maximum amplification factor of 3.7 at station 1, which is 53% higher than the value obtained there with station 3 as the reference. Furthermore, depending on the reference site we take, stations 4, 5, 6, and 7 may appear either amplified (with site 8 as reference) or deamplified (with site 3 as reference). These results clearly reveal the fundamental problem of the SRM, which is its strong dependence on the reference site. Choosing a reference is not that intuitive and the interpretation of results may significantly change with that choice. For instance, in our exercise, a reference site chosen in a deamplified area will tend to overestimate the regional amplification.

Results yielded by the MRM using the same 8 stations are displayed in Figure 5 (squares). When compared with those obtained with the same technique but using the 400 stations (black dots, Figures 4 and 5), they confirm the robustness of this approach. Despite the dramatic reduction of the stations density (i.e., 98% reduction), the amplification values with a few stations remain stable and within 20% of the values obtained from the

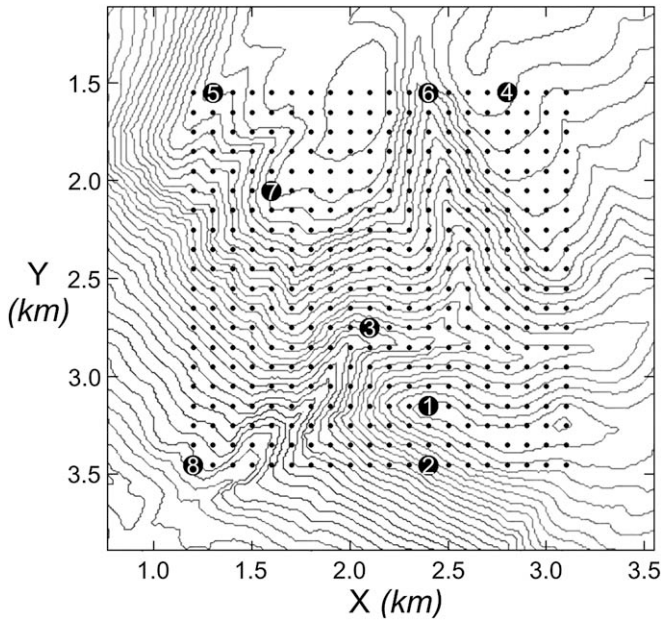

Figure 4. Zoom in on the complete seismic array of 400 stations (small black dots) superimposed on the LSBB topographic model. Indicated by numbered black circles are 8 selected stations, which were used to compare SRM and MRM site-effect estimates (see Figure 5).

absolute regional median. Even if the amounts of stations in both arrays are so different, the geometry of the arrays captures the essential topology of the free surface, thus sampling the whole variety of topographic features. This condition makes the MRM more robust than the SRM for calculating amplification factors. Furthermore, it can be easily and reliably done even with a few stations. Due to the statistical basis of the MRM, this method works best when both the amplification level 1 is covered by the stations array, and when the number of the deamplified stations is about the same as the number of the amplified ones. The best strategy to design the array geometry is to cover the valleys, the slopes and the summits with approximately the same number of the stations.

To quantitatively compare the stability of both methods in a more general sense, we perform a mathematical test under extreme conditions. We quantify the ability of each method to estimate randomly generated target amplification factors ranging between 0.1 and 10 with an absolute reference level equal to 1. To keep field-like conditions, only 7 amplitudes (i.e., seven stations) are used for the calculation. The distribution between amplified and deamplified values is randomly generated, that is, the number of amplified-stations (and thus deamplified as well) is randomly set between 1 and 7, and all 7 amplitudes are random values respecting such a distribution between amplified and deamplified stations. We performed 1,000 realizations, each one based on a different set of 7 amplitudes. Due to the random-distribution conditions, the median reference level computed by the MRM exceeds ± 50% of the absolute reference level of 1 in 45% of the realizations. To meet a

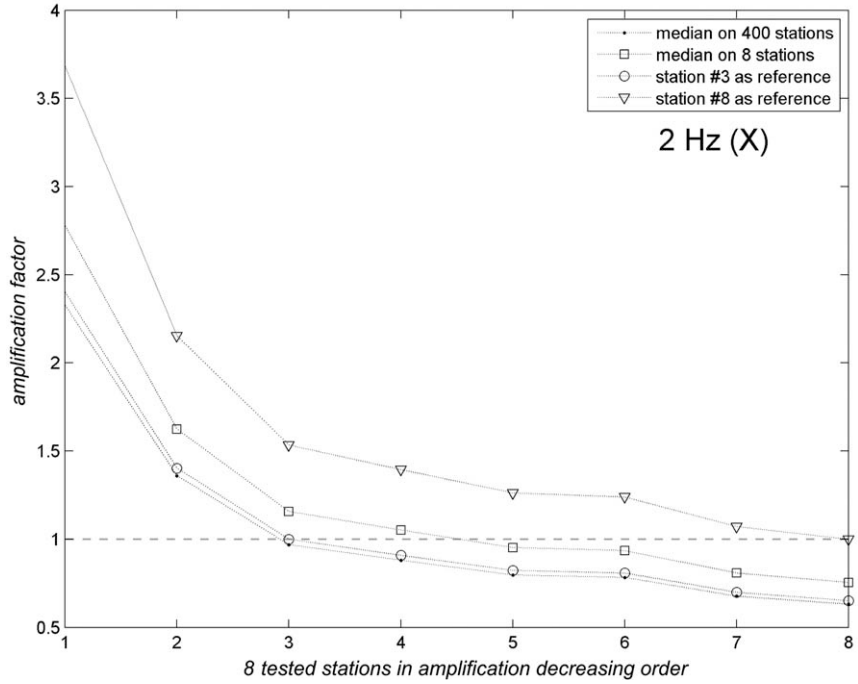

Figure 5. Comparison of the amplification factors obtained for 8 selected stations (shown in Figure 4) with the SRM (circles: using station #3 as reference; triangles: using station #8 as reference) and the MRM (squares: using the median of the 8 stations as reference; dots: using the median of all 400 stations as reference).

similar condition for the SRM and make the comparison between both methods possible, the choice of the SRM reference station has been forced to keep the same amount of realizations (i.e., 45%) whose single reference level exceeds ± 50% of the absolute reference level of 1. Despite such extreme conditions, the average deviation between the MRM estimates and the absolute amplification factor is ± 40%, while the corresponding deviation for the SRM estimates exceeds ± 100% of the target. This shows that even in bad array design conditions and without any a priori knowledge about site effects in the studied area, the MRM is much more robust than the SRM. Chávez-García et al. (1990) determined from experimental data that the total uncertainty in their SRM estimates was about a factor 2. This value is equivalent to our estimate for the SRM where deviations exceeded 100% of the target.

INFLUENCE OF TOPOGRAPHIC ROUGHNESS

To illustrate the advantages of 3-D calculations over simple 2-D analysis, Figure 6 shows MRM amplification factors produced by an isotropic source located 5 km depth to the southwestern of the model (see red circle in Figure 2a). Figure 6a shows results obtained considering only the first order slope of the Albion plateau (i.e., excluding valleys, which yields a 2-D free-surface geometry). With such a simplified topography, the problem may be considered

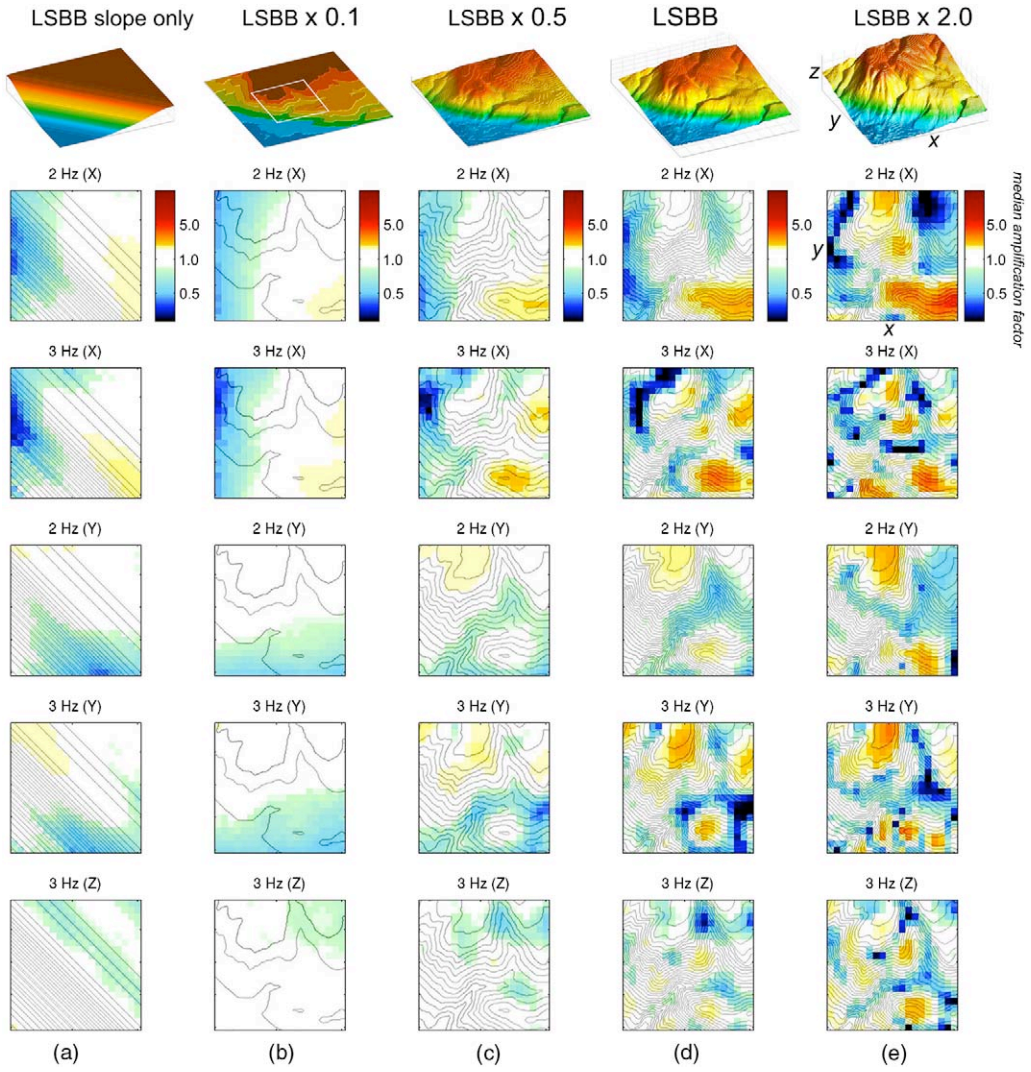

Figure 6. MRM amplification factors (color scale) for homogeneous models with realistic topography derived from the original LSBB model: (a) first order slope; and real topography multiplied by a scaling factor equal to (b) 0.1, (c) 0.5, (d) 1.0, and (e) 2.0. Receivers are spread out regularly within the white square area of the topographic model in column b, with one station every 100 m. The isotropic source is located in the southwestern corner at 5 km depth (see Figure 1). The maximum frequency of these simulations is 5 Hz. Elevation contour lines are every 20 m except for column e, where they are every 40 m.

as a 2.5-D propagation model. Only a weak and spread out amplification is observed along the main ridge, with MRM amplification factors not exceeding 2.0 at 3 Hz in the x component. Such a small level of amplification is typically observed in 2-D calculations (Geli et al. 1988). 2-D simulations can be useful to roughly determine those frequencies and components

with maximum amplification. However, as we shall see in the next paragraph, the amplification pattern is not as accurate as the one yielded by 3-D calculations, which provide more details and slightly larger amplifications over the most accentuated topographic features.

Patterns of the amplification factors may significantly change with the roughness of topography. These patterns are mainly determined by the surface steepness and differential elevations along with the wavefield frequency content. Figures 6b-e illustrates the strong effect of these factors on the seismic response of the LSBB topographic model for the same source location. To smooth (Figures 6b and 6c) or accentuate (Figure 6e) the relief, a scaling factor is applied to the real LSBB topography (Figure 6d). Site effects have different magnitudes from one model to another, even if amplification often but not always occurs on the positive (convex) reliefs and deamplification occurs on the negative (concave) reliefs. This pattern may not be true and reverse depending on the ground motion component and frequency (e.g., compare Figure 6e in both horizontal components for 2 Hz and 3 Hz at the northeastern-most ridge). Generally speaking, smooth slopes and low altitudes produce no or weak effects, while strong slopes and extreme altitudes produce medium to strong site effects so that patterns of MRM amplification factors spatially correlate with the topography shape. As expected, the maximum amplification is frequency and component dependent, which is in accordance with the previous field and numerical studies (Bouchon 1973, Geli et al. 1988, Bouchon and Barker 1996, Durand et al. 1999, Chaljub et al. 2010). Our results, obtained with the MRM, do not contradict calculations using the SRM by previous authors and suggest, in accordance with Geli et al. (1988) and Bouchon and Barker (1996), that 3-D simulations allow much more reliable amplification estimates, being closer to observed levels in field data.

INFLUENCE OF SOURCE LOCATION AND MECHANISM

The MRM amplification patterns obtained for the LSBB topography (Figure 6) may also significantly change depending on the source location. The topographic site-effects dependence on the wavefield incidence angle was already shown in 2-D by Trifunac (1972), Bouchon (1973) and Wong et al. (1977): the maximum amplification of the ground motion occurs at crests on the opposite side of the upcoming wavefield. This phenomenon should also be present in our 3-D simulations; however, given the intricate topography of the LSBB site, it may not be so easily understood. For this reason, to characterize the amplification patterns irrespective of the source location (i.e., of the wavefield incidence angle), we carried out a large amount of simulations using the LSBB topographic model with randomly generated hypocenter locations. Furthermore, to explore if those patterns depend on the kind of the incidence wavefield (i.e., P and S-waves), the exercise was completed in two parts: firstly we considered a set of 200 simulations with isotropic sources; secondly we performed 200 more simulations with randomly generated double couple focal mechanisms (i.e., strike, dip and rake, and seismic moment magnitude $M_w = 4.5$). Both sets of sources cover the entire range of back azimuths with a Gaussian distribution of incidence angles centered at 35° (incidence angles smaller than 12° and greater than 47° are poorly represented). Such restrictions on the incidence angles are due to the size of the numerical box that was limited by our current computational power. Results from our 400 simulations are summarized in Figure 7.

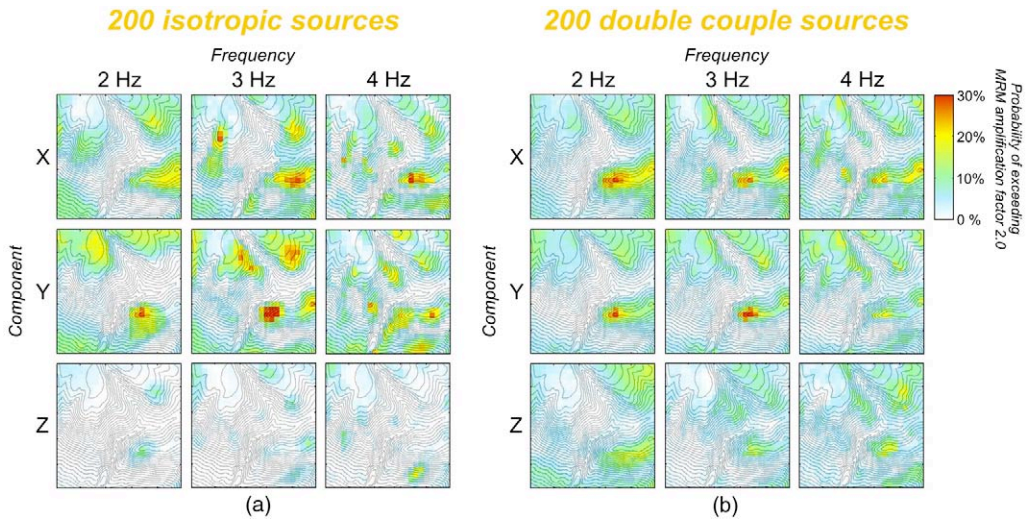

Figure 7. Probability of exceeding a MRM amplification factor of 2.0 due to topography at the LSBB Underground Laboratory (color scale) obtained from (a) 200 randomly located isotropic sources, and (b) 200 randomly located double-couple sources with random focal mechanisms. Results are reported for all three ground motion components and three different frequencies (i.e., 2 Hz, 3 Hz, and 4 Hz).

Site effects reported in Figure 7 are expressed in terms of probability of exceeding a MRM amplification factor of 2. Our simulations in the LSBB topographic model basically show that the maximum probability to overcome a factor 2 does not depend on the kind of source. While 36% is expected for isotropic sources, we found that 33% is expected for double couple sources. Moreover, general patterns yielded by both source kinds are very similar for all frequencies, with highest probabilities systematically lying over ridges and summits, especially in the horizontal components. However, detailed analysis of maxima locations reveals that the amplification peaks change their position depending on frequency, ground motion component and kind of source. The higher the frequency, the smaller we expect the characteristic length of a given ridge to amplify the ground motion. This means that only some wavelengths are suitable to amplify the ground motion in a given topographic feature. This may be seen on the y component for both source sets, where maximum probabilities happen specifically at 3 Hz over the central ridge. Site effect discrepancies between isotropic and double couple sources, which can be specially seen on the z (vertical) component, may be due to the larger range of wavefield polarizations radiated from the point dislocation sources. The wavefield due to these sources, besides P-waves, also contains a large amount of S-wave energy with different polarizations. This is not the case for isotropic sources and is the reason why we consider that results on Figure 7b are more realistic than those on Figure 7a.

Our maps help to define the areas where the amplification due to the topography is more likely to occur, even though this effect is far from being systematic. Our numerical tests show

that the amplification level in a given site may be significant, but only for specific sources. In the area of the LSBB site, 33% of the double couple sources we tested exceed an amplification factor 2 on one component at a given frequency, while only 8% exceed a factor 3. However, these percentages may rise up to ~100% for a factor 2 at the sharpest topographic features when considering the maximum of the three components for all frequencies (see Maufroy 2010). The 400 simulations we analyzed show that the topographic site effect always occurs at the scale of the most prominent topographic features, but is never systematic at the scale of single observational points. The location and extent of the amplification areas, as well as the component of ground motion where the amplification occurs, strongly depend on the source location, focal mechanism and frequency. This demonstrates that such a source-dependent variability should be considered as a first-order statistical parameter to significantly improve the reliability of the site effect assessments on intricate topographic areas.

CONCLUSIONS AND PERSPECTIVES

Results from our numerical tests are in general agreement with those obtained in numerous studies (Geli et al. 1988, Kawase and Aki 1990, Bouchon and Barker 1996, Chávez-García et al. 1996, Durand et al. 1999, Gaffet et al. 2000, Assimaki et al. 2005a, 2005b). The range of amplification values due to the topography we found with the statistical MRM is also coherent with values most commonly reported in the literature. We have demonstrated that the MRM provides reliable characterization and quantification of the site effects in mountainous areas. Furthermore, it avoids the critical choice of a reference site. Our results for both isotropic and double-couple point sources show that the number of stations is not critical when using the MRM. Considering regularly-spaced arrays, a 94% reduction of the number of stations (i.e., from 400 to 25 stations) yield MRM site effect estimates in all sites within 5% of the values obtained from the absolute regional median. Even in a more extreme (realistic) case, with irregularly located sites and using a 98% station reduction (i.e., only 8 stations), we found MRM site effect estimates systematically within 20% of the values obtained from the absolute regional median, which proves the robustness of the method and its great potential for field experiments. In contrast, for the same tests and depending on the reference site, the standard SRM yielded overestimates of the amplification factors greater than 50% in some areas, and up to 100% in specific sites.

The simulations we carried out show that finding the no-amplified level in the studied area is a senseless task, since the location of such level may significantly change depending on the frequency, ground motion component, source location and mechanism. Thus it is strictly impossible to define a single reference site valid for the whole of possible seismic scenarios and frequency bands. For this reason, the MRM is much more suitable to solve the problem than the SRM. Using the MRM to compute amplification factors in areas with intricate topography brings the possibility of comparison between different study cases, since the reference is not a specific site but the median ground motion of the entire area of interest.

As expected, our numerical simulations considering the high-resolution topographic map of the inter-Disciplinary Underground Science and Technology Laboratory (i-DUST, LSBB) show that topographic site effects are always present at the scale of hills and that their patterns correlate pretty well with the shape of the topography. However, due to the source variability, they are not systematic at the scale of single observational points. These results are in

agreement with observations by Spudich et al. (1996), where a station located at a summit experienced remarkably dissimilar amplification levels for two different earthquakes. We thus conclude this source-dependence variability to be a first-order statistical parameter in the assessment of topographic site effects. Furthermore we determined that, for arbitrary double-couple source mechanisms and locations in the LSBB region, there is a 33% probability to exceed an amplification factor of 2 in the frequency band from 2 to 4 Hz, and an 8% probability to exceed a factor of 3 simply due to the topography, in the surroundings of the sharpest summit.

Our results further suggest a new methodological approach in field experiments, where the amount of stations is often limited. Due to the statistical basis of the MRM, this method works best when the following two conditions are met: (1) areas with amplification level 1 are covered by the stations array, and (2) the number of stations in amplified areas is about the same as the number of stations in deamplified ones. Our numerical tests show that the best strategy to fulfill these conditions when designing the array geometry is to cover (i.e., install instruments at) the summits, the valleys and the slopes with approximately the same number of stations. Under this condition, the amplification factor of 1 corresponds to the absence of site effect. We think numerical simulations including real topographies are the best way to refine the sampling strategy to be deployed in the field.

In this investigation, we have only considered point sources. Theory says that the SRM and the MRM are both valid for this source description. However, from Equation 1 we see that the SRM is no longer valid if the source contribution function significantly varies between the reference site and another site of interest. This situation may arise when the size of the source is comparable to the source-array distance. In the case of the median reference method (MRM), its failure under this condition is not so evident. This question, though not examined in this paper, must be addressed before applying the MRM whenever the point source approximation is not justified.

One of the purposes of numerical simulations is to better understand the ground motion in areas where the seismic hazard is imminent. To this end, numerical predictions should be close to real data. The complexity of the near surface geology may completely modify the pattern of site effects, for example due to seismic waves channeling, scattering or low velocity sediments. Therefore, realistic 3-D velocity models are fundamental to perform reliable site effects assessments. A good knowledge of the propagation medium at the LSBB site, including geologic, hydrologic and seismic data, is required. Recently, Maufroy (2010) performed a tomographic seismic imaging study at a hectometric resolution scale. Our next step is to integrate this structural information into the 3-D topographic model and carry out improved simulations to compare with field data.

ACKNOWLEDGEMENTS

The funding for this study was provided by the inter-Disciplinary Underground Science and Technology Laboratory (LSBB), France. The digitalization of the topography surrounding the LSBB was provided by the IGN, France. This work was granted access to the HPC resources of IDRIS under the allocation i2009046038 made by GENCI (Grand Equipement National de Calcul Intensif). This research was partly funded by UNAM through the PAPIIT grant with number IN119409.

REFERENCES

Ashford, S. A., and Sitar, N., 1997. Analysis of topographic amplification of inclined shear waves in a steep coastal bluff, *Bull. Seism. Soc. Am.* **87**, 692–700.

Assimaki, D., Gazetas, G., and Kausel, E., 2005a. Effects of local soil conditions on the topographic aggravation of seismic motion: parametric investigation and recorded field evidence from the 1999 Athens earthquake, *Bull. Seism. Soc. Am.* **95**, 1059–1089.

Assimaki, D., Kausel, E., and Gazetas, G., 2005b. Soil-dependent topographic effects: a case study from the 1999 Athens earthquake, *Earthquake Spectra* **21**, 929–966.

Bard, P.-Y., and Méneroud, J.-P., 1987. Modification du signal sismique par la topographie, cas de la vallée de la Roya (Alpes Maritimes), *Bull. liaison Labo. P. et Ch.* **150/151**, 140–151.

Bohlen, T., and Saenger, E. H., 2006. Accuracy of heterogeneous staggered-grid finite-difference modeling of Rayleigh waves, *Geophysics* **71**, T109–T115.

Boore, D. M., 1972. A note on the effect of simple topography on seismic SH waves, *Bull. Seism. Soc. Am.* **62**, 275–284.

Boore, D. M., Harmsen, S. C., and Harding, S. T., 1981. Wave scattering from a step change in surface topography, *Bull. Seism. Soc. Am.* **71**, 117–125.

Borcherdt, R. D., 1970. Effects of local geology on ground motion near San Francisco Bay, *Bull. Seism. Soc. Am.* **60**, 29–61.

Bouchon, M., 1973. Effect of topography on surface motion, *Bull. Seism. Soc. Am.* **63**, 615–632.

Bouchon, M., and Barker, J. S., 1996. Seismic response of a hill: the example of Tarzana, California, *Bull. Seism. Soc. Am.* **86**, 66–72.

Çelebi, M., 1987. Topographical and geological amplifications determined from strong-motion and aftershocks records of the 3 march 1985 Chile earthquake, *Bull. Seism. Soc. Am.* **77**, 1147–1167.

Chaljub, E., Moczo, P., Tsuno, S., Bard, P.-Y., Kristek, J., Käser, M., Stupazzini, M., and Kristekova, M., 2010. Quantitative comparison of four numerical predictions of 3-D ground motion in the Grenoble valley, France, *Bull. Seism. Soc. Am.* **100**, 1427–1455.

Chávez-García, F. J., Pedotti, G., Hatzfeld, D., and Bard, P.-Y., 1990. An experimental study of site effects near Thessaloniki (Northern Greece), *Bull. Seism. Soc. Am.* **80**, 784–806.

Chávez-García, F. J., Sánchez, L. R., and Hatzfeld, D., 1996. Topographic site effects and HVSR, a comparison between observations and theory, *Bull. Seism. Soc. Am.* **86**, 1559–1573.

Chávez-García, F. J., Rodríguez, M., Field, E. H., and Hatzfeld, D., 1997. Topographic site effects, a comparison of two nonreference methods, *Bull. Seism. Soc. Am.* **87**, 1667–1673.

Cruz-Atienza, V. M., 2006. Rupture dynamique des failles non-planaires en différences finies, Ph.D. thesis, University of Nice Sophia-Antipolis.

Cruz-Atienza, V. M., Virieux, J., and Aochi, H., 2007a. 3-D finite-difference dynamic-rupture modeling along non-planar faults, *Geophysics* **72**, SM123–SM137.

Cruz-Atienza, V. M., Virieux, J., Khors-Sansorny, C., Sardou, O., Gaffet, S., and Vallée, M., 2007b. Estimation quantitative du PGA sur la Côte d'Azur, *7ème Colloque National, Association Française du Génie Parasismique (AFPS)*, p. 8, Ecole Centrale Paris, France.

Davis, L. L., and West, L. R., 1973. Observed effects of topography on ground motion, *Bull. Seism. Soc. Am.* **63**, 283–298.

Durand, S., Gaffet, S., and Virieux, J., 1999. Seismic diffracted waves from topography using 3-D discrete wavenumber-boundary integral equation simulation, *Geophysics* **64**, 572–578.

Field, E. H., and Jacob, K. H., 1995. A comparison and test of various site-response estimation techniques, including three that are not reference-site dependent, *Bull. Seism. Soc. Am.* **85**, 1127–1143.

Gaffet, S., Cultrera, G., Dietrich, M., Courboulex, F., Marra, F., Bouchon, M., Caserta, A., Cornou, C., Deschamps, A., Glot, J.-P., and Guiguet, R., 2000. A site effect study in the Verchiano valley during the 1997 Umbria-Marche (Central Italy) earthquakes, *J. Seism.* **4**, 525–541.

Geli, L., Bard, P.-Y., and Jullien, B., 1988. The effect of topography on earthquake ground motion: a review and new results, *Bull. Seism. Soc. Am.* **78**, 42–63.

Hartzell, S. H., Carver, D. L., and King, K. W., 1994. Initial investigation of site and topographic effects at Robinwood Ridge, California, *Bull. Seism. Soc. Am.* **84**, 1336–1349.

Kawase, H., and Aki, K., 1990. Topography effect at the critical SV-wave incidence: possible explanation of damage pattern by the Whittier Narrows, California, earthquake of 1 October 1987, *Bull. Seism. Soc. Am.* **80**, 1–22.

Lee, S.-J., Komatitsch, D., Huang, B.-S., and Tromp, J., 2009a. Effects of topography on seismic wave propagation: An example from northern Taiwan, *Bull. Seism. Soc. Am.* **99**, 314–325.

Lee, S.-J., Chan, Y.-C., Komatitsch, D., Huang, B.-S., and Tromp, J., 2009b. Effects of realistic surface topography on seismic ground motion in the Yangminshan region of Taiwan based upon the spectral-element method and LiDAR DTM, *Bull. Seism. Soc. Am.* **99**, 681–693.

Maufroy, E., 2010. Caractérisation et modélisation numérique de l'effet de site topographique 3-D: application à la Grande Montagne de Rustrel, Vaucluse, *Ph.D. thesis*, University of Nice Sophia-Antipolis, France.

Montalvo-Arrieta, J. C., Sánchez-Sesma, F. J., and Reinoso, E., 2002. A virtual reference site for the valley of Mexico, *Bull. Seism. Soc. Am.* **92**, 1847–1854.

Nechtschein, S., Bard, P.-Y., Gariel, J.-C., Méneroud, J.-P., Dervin, P., Cushing, M., Gaubert, C., Vidal, S., and Duval, A.-M., 1995. A topographic effect study in the Nice region, *Proceedings of the fifth International Conference on Seismic Zonation*, Nice, France, 1067–1074.

Pedersen, H. A., Le Brun, B., Hatzfeld, D., Campillo, M., and Bard, P.-Y., 1994. Ground-motion amplitude across ridges, *Bull. Seism. Soc. Am.* **84**, 1786–1800.

Poppeliers, C., and Pavlis, G. L., 2002. The seismic response of a steep slope: high-resolution observations with a dense, three-component seismic array, *Bull. Seism. Soc. Am.* **92**, 3102–3115.

Rogers, A. M., Katz, L. J., and Bennett, T. J., 1974. Topographic effects on ground motion for incident P waves: a model study, *Bull. Seism. Soc. Am.* **64**, 437–456.

Sanchez-Sesma, F. J., and Campillo, M., 1991. Diffraction of P, SV, and Rayleigh waves by topographic features: a boundary integral formulation, *Bull. Seism. Soc. Am.* **81**, 2234–2253.

Spudich, P., Hellweg, M., and Lee, W. H. K., 1996. Directional topographic site response at Tarzana observed in aftershocks of the 1994 Northridge, California, earthquake: implications for mainshock motions, *Bull. Seism. Soc. Am.* **86**, S193–S208.

Steidl, J. H., Tumarkin, A. G., and Archuleta, R. J., 1996. What is a reference site?, *Bull. Seism. Soc. Am.* **86**, 1733–1748.

Trifunac, M. D., 1972. Scattering of plane sh waves by a semi-cylindrical canyon, *Earthquake Engng. Struct. Dyn.* **1**, 267–281.

Trifunac, M. D., and Hudson, D. E., 1971. Analysis of the Pacoima dam accelerogram, San Fernando, California, earthquake of 1971, *Bull. Seism. Soc. Am.* **61**, 1393–1141.

Tucker, B. E., King, J. L., Hatzfeld, D., and Nersesov, I. L., 1984. Observations of hard-rock site effects, *Bull. Seism. Soc. Am.* **74**, 121–136.

Umeda, Y., Kuroiso, A., Ito, K., and Muramatu, I., 1987. High accelerations produced by the Western Nagano Prefecture, Japan, earthquake of 1984, *Tectonophysics* **141**, 335–343.

Wilson, D. C., and Pavlis, G. L., 2000. Near-surface site effects in crystalline bedrock: a comprehensive analysis of spectral amplitudes determined from a dense, three-component seismic array, *Earth Interactions* **4**, 1–31.

Wong, H. L., 1982. Effect of surface topography on the diffraction of P, SV, and Rayleigh waves, *Bull. Seism. Soc. Am.* **72**, 1167–1183.

Wong, H. L., Trifunac, M. D., and Westermo, B., 1977. Effects of surface and subsurface irregularities on the amplitudes of monochromatic waves, *Bull. Seism. Soc. Am.* **67**, 353–368.

(Received 28 October 2010; accepted 23 January 2012)